

Dissociation cross sections of ground state and excited charmonia with light mesons in the quark model

T. Barnes,^{1,2} E. S. Swanson,^{3,4} C.-Y. Wong,¹ and X.-M. Xu¹

¹Physics Division, Oak Ridge National Laboratory, Oak Ridge, Tennessee 37831, USA

²Department of Physics and Astronomy, University of Tennessee, Knoxville, Tennessee 37996, USA

³Department of Physics and Astronomy, University of Pittsburgh, Pittsburgh, Pennsylvania 15260, USA

⁴Thomas Jefferson National Accelerator Facility, Newport News, Virginia 23606, USA

(Received 20 February 2003; published 29 July 2003)

We present numerical results for the dissociation cross sections of ground state, and orbitally and radially excited charmonia in collisions with light mesons. Our results are derived using the nonrelativistic quark model, so all parameters are determined by fits to the experimental meson spectrum. Examples of dissociation into both exclusive and inclusive final states are considered. The dissociation cross sections of several $C = (+)$ charmonia may be of considerable importance for the study of heavy ion collisions, since these states are expected to be produced more copiously than J/ψ . The relative importance of the productions of ground-state and orbitally excited charmed mesons in a pion-charmonium collision is demonstrated through the \sqrt{s} -dependent charmonium dissociation cross sections.

DOI: 10.1103/PhysRevC.68.014903

PACS number(s): 25.75.Nq, 12.39.Jh, 13.75.Lb

I. INTRODUCTION

The interactions of mesons in systems containing both light and heavy quarks have long been of interest to hadron physicists. For example, some models predict that the open-charm D and \bar{D} mesons have sufficiently attractive residual strong interactions with nucleons to form “charmed nuclei” [1,2]. Charmed hadron bound states may exist in other systems as well; long ago, Novikov *et al.* speculated that the nominal 3^3S_1 $c\bar{c}$ state $\psi(4040)$ might actually be a quasi-nuclear “molecule” bound state of a $D^*\bar{D}^*$ pair [3]. Several quark-model studies have shown that $Q^2\bar{q}^2$ mesons should exist for sufficiently large heavy-quark mass m_Q (for a recent review, see the work by Richard [4]). In a recent “pedagogical” application, the $m_Q \rightarrow \infty$ limit of the $Q^2\bar{q}^2$ heavy-light system (the so-called $\mathcal{B}\mathcal{B}$ system) has been used as a theoretical laboratory for the study of nuclear forces, and nuclear potential energy curves have been derived using the nonrelativistic quark model [5] and lattice gauge theory [6].

Recently, further interest in the interactions of light- and heavy-quark mesons has arisen in the context of heavy-ion collisions and the search for the quark-gluon plasma (QGP). One signature proposed for the identification of a QGP [7] is the suppression of the rate of formation of the J/ψ and other $c\bar{c}$ bound states. The long-ranged linear confining potential between a $c\bar{c}$ pair would purportedly be screened by a QGP, so a $c\bar{c}$ pair produced in the collision would be more likely to separate than to populate bound $c\bar{c}$ resonances.

Direct experimental confirmation of such a suppression can be detected, for example, through the observation of lepton pairs from the decay $J/\psi \rightarrow \ell^+\ell^-$. The simplest interpretation of an observed $J/\psi \rightarrow \ell^+\ell^-$ signal would be to assume that all J/ψ mesons survive until they decay outside the interaction region. However, if dissociation reactions such as $\pi + J/\psi \rightarrow D^*\bar{D}$ and $\rho + J/\psi \rightarrow D\bar{D}$ are important, the inter-

pretation of the experiment is more complicated; a weak J/ψ signal might simply be due to dissociation through such “comover absorption” processes. The actual size of these low-energy charmonium dissociation cross sections is currently very controversial, and their evaluation is the subject of this paper.

II. APPROACHES

A very wide range of theoretical estimates of low-energy charmonium dissociation cross sections has been reported in the literature, largely due to different assumptions for the dominant scattering mechanisms. We will briefly review the three main approaches used before presenting new results from our quark-model calculations.

A. Quark interchange

Quark-model calculations of charmonium–light hadron cross sections were first reported by Martins, Blaschke, and Quack [8], who used a quark-interchange model [9] to treat $\pi + J/\psi$ collisions. This reference used standard quark-model one-gluon exchange (OGE) forces (spin-spin hyperfine and color Coulomb), augmented by a color-independent confining force that was assumed to act only between $q\bar{q}$ pairs (no qq or $\bar{q}\bar{q}$ anticonfining interaction). Since the color Coulomb terms experience destructive interference between diagrams (due to color factors), and the large mass of the charm quark makes the hyperfine term rather weak, Martins *et al.* concluded that OGE forces alone give rather small cross sections; they estimated a cross section for $\pi + J/\psi \rightarrow D^*\bar{D} + \text{H.c.} + D^*\bar{D}^*$ of ≈ 0.3 mb at $\sqrt{s} \approx 4.2$ GeV. However their color-independent, $q\bar{q}$ -only confining interaction had no color factor cancellation, and so gave a much larger peak cross section of ≈ 7 mb near 4.1 GeV. These two exclusive processes ($D^*\bar{D} + \text{H.c.}$ and $D^*\bar{D}^*$) were found to peak quite close to threshold, and then fell rapidly with in-

creasing invariant mass due to suppression from the assumed Gaussian meson wave functions. (See Fig. 2 of Ref. [8].) Subsequently, Wong *et al.* [11] applied the same approach to this problem, *albeit* with the conventional quark-model $\lambda \cdot \lambda$ dependence for all terms in the interquark Hamiltonian, including the linear confining potential. The interaction terms assumed were again color Coulomb, spin-spin hyperfine, and linear scalar confinement. The destructive interference between *all* diagrams, due to zero-sum color factors, led to a rather smaller $\pi + J/\psi \rightarrow D^* \bar{D} + \text{H.c.} + D^* \bar{D}^*$ cross section, with a rather broad peak of roughly 1 mb near 4.1 GeV. Wong *et al.* also considered $\pi + \psi'$, $\rho + J/\psi$, and $\rho + \psi'$ dissociation, and found that these cross sections are much larger than $\pi + J/\psi$ near threshold, due to more favorable kinematics. The $\rho + (c\bar{c})$ processes are exothermic, and so actually diverge at threshold. Finally, Wong *et al.* studied the importance of the so-called “post-prior ambiguity” [12] in these calculations; the use of exact $q\bar{q}$ Hamiltonian wave functions in the present paper eliminates much of this systematic effect, but an important discrepancy remains due to the use of relativistic phase space and physical masses.

Shuryak and Teaney [13] gave a comparable rough estimate of ≈ 1.2 mb for a low-energy $\pi + J/\psi$ cross section driven by the nonrelativistic quark-model’s spin-spin interaction. Actually the specific process they considered, $\pi + J/\psi \rightarrow \eta_c + \rho$, is zero at Born order due to a vanishing color factor; color was not incorporated in their estimate.

B. Meson exchange

Charmonium–light hadron scattering can also take place through t -channel meson exchange. This mechanism was first discussed by Matinyan and Müller [14], who were motivated to study $\pi + J/\psi$ inelastic scattering by the great discrepancy between the ca. 7 mb quark-model result of Martins *et al.* [8] and the very small low-energy cross sections found using the Peskin-Bhanot approach [15]. In the meson-exchange picture, charmonium dissociation reactions proceed through t -channel exchange of charmed mesons such as D and D^* . Matinyan and Müller assumed only D exchange, and found mb-scale cross sections for the two low-energy dissociation processes $\pi + J/\psi \rightarrow D^* \bar{D} + \text{H.c.}$ and $\rho + J/\psi \rightarrow D \bar{D}$.

This work has since been generalized to other t -channel exchanges and effective meson Lagrangians. Lin, Ko, and Zhang had previously proposed an SU(4) flavor symmetric vector-pseudoscalar meson effective Lagrangian which they had applied to open-charm meson scattering [16]. Application of this same Lagrangian to the $\pi + J/\psi$ dissociation reaction $\pi + J/\psi \rightarrow D^* \bar{D} + \text{H.c.}$ gave a rather large cross section of ≈ 20 –30 mb for $\sqrt{s} = 4$ –5 GeV [17]; this was much larger than the D -exchange results of Matinyan and Müller, due to new three- and four-meson vertices in their effective Lagrangian. Haglin [18] introduced a similar SU(4) symmetric meson Lagrangian, and also found rather large cross sections of 5–10 mb for $\sqrt{s} = 4$ –6 GeV for many low-energy charmonium dissociation reactions (see, for example, Fig. 2 of Ref. [18]). Subsequent work by Haglin and Gale [19]

showed that the $\pi + J/\psi$ total inelastic cross section would reach an extremely large value of roughly 100 mb at $\sqrt{s} = 5$ GeV, and $\rho + J/\psi$ a fantastic ≈ 300 mb (with both still increasing) in this model, assuming pointlike hadron vertices. Similar large $\pi + J/\psi$ and $\rho + J/\psi$ cross sections have been reported by Oh, Song and Lee in pointlike meson exchange models [20].

Navarra *et al.* [21] have recently questioned the assumption of flavor SU(4) symmetry; keeping only isospin symmetry, they find rather smaller cross sections for $\pi + J/\psi \rightarrow D^* \bar{D} + \text{H.c.}$, ca. 20–25 mb at $\sqrt{s} = 5$ GeV. They confirm that D^* exchange is much more important numerically in meson exchange models than the D exchange originally assumed by Matinyan and Müller.

Of course, it is also incorrect to assume pointlike hadron form factors. This has been noted both by Lin and Ko [17] and Haglin and Gale [19]. Both collaborations investigated the effect of assuming monopole forms for the effective three-meson vertices, and concluded that the predicted cross sections were greatly reduced (once again to typically 1–10 mb scales) with plausible vertex functions. (See, for example, Fig. 4 of Ref. [17] and Fig. 7 of Ref. [19].) Accurate calculations of hadronic vertex functions are clearly of crucial importance for meson-exchange models of charmonium dissociation. Some results for these form factors, obtained from QCD sum rules, have been published by Navarra *et al.* [22,23].

C. Diffractive model

A high-energy diffractive description of scattering of heavy quarkonia which was developed in 1979 by Peskin and Bhanot [24] has also been applied to the calculation of charmonium cross sections. It should be stressed that this method is only justified at high energies [25], and then only for deeply bound $Q\bar{Q}$ systems. It is in essence a gluon-sea model of high-energy diffractive scattering of physically small, high-mass Coulombic bound states by light hadrons. This model predicts reasonable mb-scale cross sections for J/ψ hadronic cross sections at $\sqrt{s} \geq 10$ GeV [24,15,26,27]. At low energies, however, this mechanism taken in isolation predicts extremely small (sub- μb) cross sections for $J/\psi + \pi$ and $J/\psi + N$ (see Fig. 2 of Ref. [27]). Presumably, this means that the Peskin-Bhanot diffractive scattering mechanism is unimportant in the low-energy regime of greatest relevance to QGP searches, and other mechanisms such as quark interchange and meson exchange dominate $c\bar{c}$ strong interactions at these low energies. Indeed, a recent comparison [28] with lattice gauge computations shows that the operator product expansion breaks down for quark masses below roughly 100 GeV, and therefore the Peskin model is inapplicable to light and charmed hadronic physics.

Redlich *et al.* [29] have argued that these diffractive cross sections are actually accurate at low energies, and if combined with vector dominance, these can account for the experimental $\gamma N \rightarrow J/\psi + N \rightarrow$ open-charm cross section. Hüfner *et al.* [26], however, argue that this test is misleading, as the assumption of vector dominance through the J/ψ

alone is unrealistic for these processes. Since the ψ' is much closer to open charm threshold than the J/ψ , and is predicted to have larger dissociation cross sections to open charm, this is clearly a potential source of inaccuracy for any J/ψ -only vector dominance model.

Finally, QCD sum rule calculations have been performed [30], which find a much larger low-energy cross section than the diffraction model of Ref. [15], and are in rough agreement with quark-interchange results near threshold. Although there is approximate agreement of scale at low energies, the sum rule results find that the exclusive cross sections increase monotonically with increasing energy. We believe that this is incompatible with hadronic form factors, which may require the inclusion of higher-dimensional operators in the sum rule calculations.

D. Synopsis

Clearly, the scale of charmonium dissociation cross sections at low energies remains an open question. Neither the experimental values nor the dominant scattering mechanisms have been convincingly established. In this currently rather obscure situation we can best proceed by deriving the predictions of the various models and searching for the least ambiguous comparisons with experiment, in as unbiased a manner as possible. Here we attempt to contribute to this research through a careful and detailed study of the predictions of one of the theoretical approaches, the quark-interchange model.

III. QUARK-INTERCHANGE MODEL

The Born-order quark-interchange model approximates hadron-hadron scattering as due to a single interaction of the standard quark-model interaction Hamiltonian H_I between all constituent pairs in different hadrons [9]. In the current study we specialize to quark interactions that are simple potentials times spin and color factors,

$$H_I = (v_{Coul}(r) \mathbf{I} + v_{conf}(r) \mathbf{I} + v_{ss}(r) \vec{S}_i \cdot \vec{S}_j) T^a \cdot T^a. \quad (1)$$

The potentials are the standard quark-model color Coulomb, linear confinement, and OGE spin-spin hyperfine terms, $v_{Coul} = \alpha_s/r$, $v_{conf} = -3br/4$, and $v_{ss} = -(8\pi\alpha_s/9m_i m_j) \delta_\sigma(\vec{r})$. [The Gaussian-regularized delta function is $\delta_\sigma(\vec{r}) = \sigma^3/\pi^{3/2} \cdot e^{-\sigma^2 r^2}$.]

Since this Hamiltonian is $T^a \cdot T^a$ in color space, quark line rearrangement is required to give nonzero scattering amplitudes between initial and final color-singlet hadrons at leading order in H_I . In the case of $q\bar{q}$ meson-meson scattering, this Born-order amplitude is given by the sum of the four “quark Born diagrams” shown in Fig. 1. Each interaction in each diagram has an associated “signature” fermion permutation phase, color factor \mathcal{C} , spin matrix element \mathcal{S} , and a spatial overlap integral \mathcal{I} . The evaluation of these various factors is discussed in detail in Ref. [9]. There are several simplifications in $q\bar{q}$ meson-meson scattering; the signature phase is always (-1) , the flavor factor is diagram indepen-

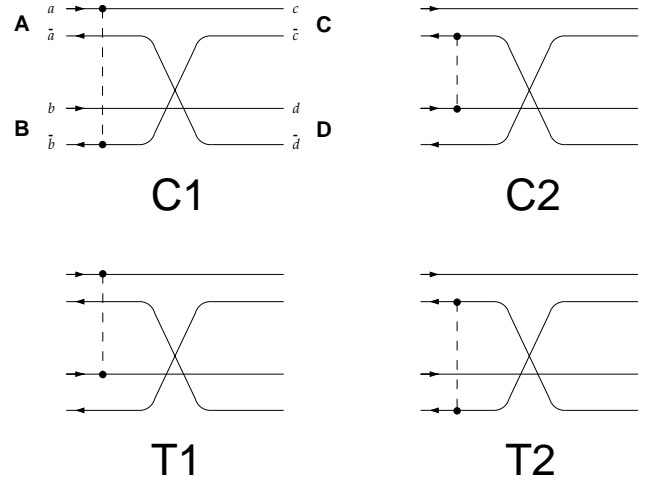


FIG. 1. The four quark-interchange meson-meson scattering diagrams in the “prior” formalism.

dent (and is unity here), and the color factors are $(-4/9)$ (capture) and $(+4/9)$ (transfer). The full meson-meson T matrix is given by the sum of color Coulomb, linear confinement, and OGE spin-spin T -matrix elements, each of the form

$$T_{fi}^{AB \rightarrow CD} = (-1) \mathcal{F} \{ (-4/9) \langle \mathcal{S} \otimes \mathcal{I} \rangle_{C_1} + (-4/9) \langle \mathcal{S} \otimes \mathcal{I} \rangle_{C_2} + (+4/9) \langle \mathcal{S} \otimes \mathcal{I} \rangle_{T_1} + (+4/9) \langle \mathcal{S} \otimes \mathcal{I} \rangle_{T_2} \}. \quad (2)$$

The angle brackets refer to the fact that the spin- and space-matrix elements do not always factor, and must in general be evaluated using a Clebsch-Gordon series. (This complication applies to spin-triplet, orbitally excited mesons.) To evaluate the cross section for a given reaction at a given energy, we first evaluate the overlap integrals (given below) for each set of orbital magnetic quantum numbers, $\langle L_C, L_{Cz}; L_D, L_{Dz} | \mathcal{I} | L_A, L_{Az}; L_B, L_{Bz} \rangle$, using an adaptive Monte Carlo technique. In this method we fix $\vec{A} = A\hat{z}$, so the overlap integrals are functions of Ω_C . (The magnitudes of A and C are determined from \sqrt{s} and the physical meson masses using relativistic kinematics.) We then evaluate spherical harmonic moments $c_{lm} = \int d\Omega_C Y_{lm}^*(\Omega_C) \mathcal{I}(\Omega_C)$ of the overlap integrals, for each diagram and interaction, usually up to $l=4$. These spatial overlap integrals are then combined with the spin matrix elements $\langle S_C, S_{Cz}; S_D, S_{Dz} | \mathcal{S} | S_A, S_{Az}; S_B, S_{Bz} \rangle$ of I and $\vec{S}_i \cdot \vec{S}_j$ in a Clebsch-Gordon series to form the full T -matrix element

$$T_{fi}^{AB \rightarrow CD} = \langle J_C, J_{Cz}; J_D, J_{Dz} | T | J_A, J_{Az}; J_B, J_{Bz} \rangle. \quad (3)$$

Polarized cross sections are then given by

$$\sigma_{fi}^{AB \rightarrow CD} = \frac{4E_A E_B E_C E_D}{s} \frac{|\vec{P}_C|}{|\vec{P}_A|} \int d\Omega_C |T_{fi}^{AB \rightarrow CD}|^2 \quad (4)$$

and the unpolarized cross sections given here are determined by summing over magnetic quantum numbers as usual.

Since our H_I consists of simple potentials, it is convenient to evaluate the overlap integrals in real space. (In most recent studies we evaluated these overlap integrals in momentum space, since they can be conveniently expressed as convolutions of the quark-quark momentum-space T matrix with external meson wave functions; see, for example, Ref. [10]. The real-space overlap integrals, which may be obtained by introducing Fourier transforms in Eqs.(1)–(4) of Ref. [10] for the special case $T_{f_i}(\vec{q}, \vec{p}_1, \vec{p}_2) = T_{f_i}(\vec{q})$, are

$$\begin{aligned} \mathcal{I}_{C_1} = & \int \hat{d}^9x \psi_A(\vec{x}_A) \psi_B(\vec{x}_B) \psi_C^*(\vec{r}) \psi_D^*(\vec{x}_A + \vec{x}_B - \vec{r}) v(r) \\ & \times \exp \left\{ -\frac{i}{2}(\vec{A} + \mu_C \vec{C}) \cdot \vec{x}_A - \frac{i}{2}(\vec{A} - \mu_D \vec{C}) \cdot \vec{x}_B + i\vec{A} \cdot \vec{r} \right\}, \end{aligned} \quad (5)$$

$$\begin{aligned} \mathcal{I}_{C_2} = & \int \hat{d}^9x \psi_A(\vec{x}_A) \psi_B(\vec{x}_B) \psi_C^*(\vec{x}_A + \vec{x}_B - \vec{r}) \psi_D^*(\vec{r}) v(r) \\ & \times \exp \left\{ +\frac{i}{2}(\vec{A} - \mu_C \vec{C}) \cdot \vec{x}_A + \frac{i}{2}(\vec{A} + \mu_D \vec{C}) \cdot \vec{x}_B \right. \\ & \left. - i\vec{A} \cdot \vec{r} \right\}, \end{aligned} \quad (6)$$

$$\begin{aligned} \mathcal{I}_{T_1} = & \int \hat{d}^9x \psi_A(\vec{x}_A) \psi_B(\vec{x}_B) \psi_C^*(\vec{x}_B + \vec{r}) \psi_D^*(\vec{x}_A - \vec{r}) v(r) \\ & \times \exp \left\{ -\frac{i}{2}(\vec{A} + \mu_C \vec{C}) \cdot \vec{x}_A + \frac{i}{2}(\vec{A} + \mu_D \vec{C}) \cdot \vec{x}_B + i\vec{A} \cdot \vec{r} \right\}, \end{aligned} \quad (7)$$

$$\begin{aligned} \mathcal{I}_{T_2} = & \int \hat{d}^9x \psi_A(\vec{x}_A) \psi_B(\vec{x}_B) \psi_C^*(\vec{x}_B + \vec{r}) \psi_D^*(\vec{x}_A - \vec{r}) v(r) \\ & \times \exp \left\{ +\frac{i}{2}(\vec{A} - \mu_C \vec{C}) \cdot \vec{x}_A - \frac{i}{2}(\vec{A} - \mu_D \vec{C}) \cdot \vec{x}_B + i\vec{A} \cdot \vec{r} \right\}, \end{aligned} \quad (8)$$

where the measure is $\hat{d}^9x \equiv d^3r d^3x_A d^3x_B / (2\pi)^3$. We also introduced $\mu \equiv 2m_q / (m_q + m_{\bar{q}})$, and the identities $\mu_A = \mu_B = 1$ and $\mu_C + \mu_D = 2$ were used in deriving the overlap integrals; these relations are valid for processes of the type $(n\bar{n}) + (c\bar{c}) \rightarrow (n\bar{c}) + (c\bar{n})$. The spatial wave functions above are the usual nonrelativistic quark potential model functions $\psi(\vec{r}_{q\bar{q}})$, normalized to $\int d^3r |\psi(\vec{r})|^2 = 1$. The wave functions employed in this paper to evaluate these overlap integrals are numerically determined eigenfunctions of the full quark-model Hamiltonian [with interaction given by Eq. (1)].

Since we use relativistic phase space and physical masses in evaluating our cross sections, there is a post-prior ambiguity in our results [12]. The overlap integrals given above are the ‘‘prior’’ forms, in which the H_I interaction takes place prior to rearrangement (Fig. 1). In the ‘‘post’’ form, rearrangement followed by interaction, the scattering amplitude is given by a different set of spin matrix elements and overlap integrals. The post overlap integrals for the two capture diagrams are

$$\begin{aligned} \mathcal{I}_{C_1}^{post} = & \int \hat{d}^9x \psi_A(\vec{r}) \psi_B(\vec{x}_C + \vec{x}_D - \vec{r}) \\ & \times \psi_C^*(\vec{x}_C) \psi_D^*(\vec{x}_D) v(r) \exp \left\{ +\frac{i}{2}(\vec{A} + \mu_D \vec{C}) \cdot \vec{x}_C \right. \\ & \left. - \frac{i}{2}(\vec{A} - \mu_D \vec{C}) \cdot \vec{x}_D - i\vec{C} \cdot \vec{r} \right\}, \end{aligned} \quad (9)$$

$$\begin{aligned} \mathcal{I}_{C_2}^{post} = & \int \hat{d}^9x \psi_A(\vec{x}_C + \vec{x}_D - \vec{r}) \\ & \times \psi_B(\vec{r}) \psi_C^*(\vec{x}_C) \psi_D^*(\vec{x}_D) v(r) \exp \left\{ +\frac{i}{2}(\vec{A} - \mu_C \vec{C}) \cdot \vec{x}_C \right. \\ & \left. - \frac{i}{2}(\vec{A} + \mu_C \vec{C}) \cdot \vec{x}_D + i\vec{C} \cdot \vec{r} \right\}. \end{aligned} \quad (10)$$

The transfer diagrams $T1$ and $T2$ (Fig. 1) in post and prior formalisms are identical.

IV. RESULTS

We have obtained Born-order quark-model results for (i) dissociation cross sections of ground-state and excited charmonia into exclusive final states, and (ii) total inelastic dissociation cross sections from the quark-interchange mechanism. These results assume the quark-interchange model described in the preceding section. In the quark-model Hamiltonian, we assume a quark-gluon coupling constant $\alpha_s = 0.6$, $\sigma = 0.9$ GeV in the spin-spin hyperfine term and a string tension of $b = 0.16$ in the linear confinement term. The light and charmed quark masses are taken to be 0.33 GeV and 1.6 GeV, respectively. These parameters can reproduce the $I = 2 \pi \pi S$ -wave experimental phase shifts [10], and are used in the following sections to calculate charmonium dissociation cross sections which are average values obtained with ‘‘prior’’ and ‘‘post’’ forms. Cross sections for π^+ scattering are presented in the following sections, other pion cross sections may be obtained assuming isospin symmetry.

A. Dissociation cross sections of excited charmonia

The principal mechanism for production of charmonia at small x in heavy ion collisions is thought to be the two-gluon fusion process $gg \rightarrow c\bar{c}$. One therefore expects J/ψ production to be relatively weak, since the formation of $C = (-)$ states requires an additional gluon. The $C = (+)$ mesons that have especially large gg couplings, such as η_c , χ_{c0} , and (to a lesser extent) χ_{c2} and their, as yet unidentified, radial excitations should be the dominant $c\bar{c}$ states produced. The relative strengths of $c\bar{c}$ couplings to glue are dramatically illustrated by the total widths of charmonia; the η_c and χ_{c0} total widths, thought to be due mainly to $c\bar{c} \rightarrow gg$, are two orders of magnitude larger than the J/ψ total width. Even the smaller χ_{c2} width is roughly 20 times the J/ψ width. This suggests that the production of charmonia from a quark-gluon plasma is probably dominated by these $C = (+)$ states rather than J/ψ , so the evolution of $C = (+)$ states produced

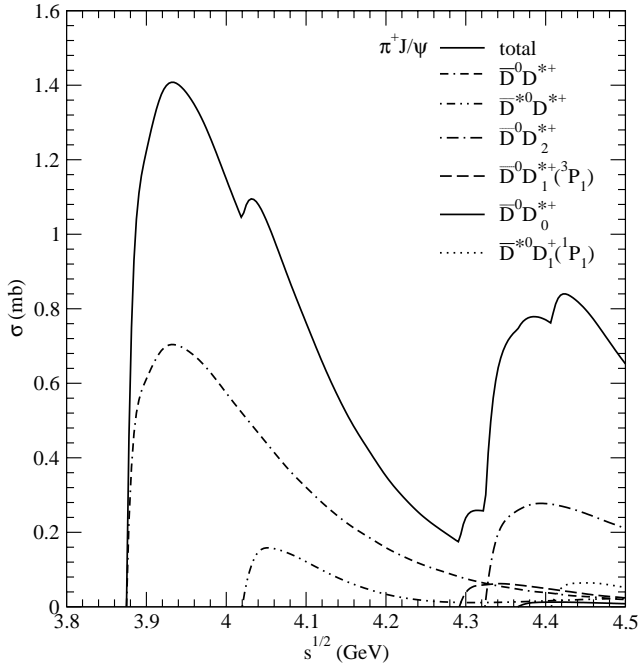


FIG. 2. Theoretical $\pi^+ J/\psi$ cross sections in the quark-interchange model. The figure shows all nonzero partial cross sections open to $\sqrt{s}=4.5$ GeV; the total cross section, obtained by summing these and their charge conjugate channels, is shown as a solid line.

in a heavy-ion collision may be more important for understanding charm production than the J/ψ . The possibility that much of the J/ψ signal originates from radiative transitions of parent χ_{cJ} states [31,32] also suggests that an understanding of the interactions of these $C=(+)$ and excited $c\bar{c}$ states with light hadrons may be of great importance for simulations of heavy flavor production in heavy ion collisions.

It is straightforward to determine the dissociation cross sections of $c\bar{c}$ states other than the J/ψ in the quark-interchange model; one simply changes the external state attached to each of the four scattering diagrams of Fig. 1. There is a technical complication with spin-triplet, orbitally excited charmonia, since the spin and space degrees of freedom do not factor trivially in these states, unlike the scattering of S -wave mesons considered previously [11]. Instead, we must evaluate overlap integrals and spin-matrix elements for each set of magnetic quantum numbers, which are then combined using the appropriate Clebsch-Gordon coefficients to give scattering amplitudes of mesons with definite J (e.g., $\pi^+ \chi_{cJ} \rightarrow \bar{D} D^*$).

B. Total π -charmonium dissociation cross sections from constituent interchange

We have evaluated the $\pi J/\psi$, $\pi \psi'$, and $\pi \chi_{cJ}$ exclusive and total cross sections up to 4.5 GeV in the center of mass frame. The six final states with nonzero couplings in the model which are open in this regime are

$$\pi^+ + c\bar{c} \rightarrow \bar{D}^0 D^{*+} + \text{c.c.}, \quad (11)$$

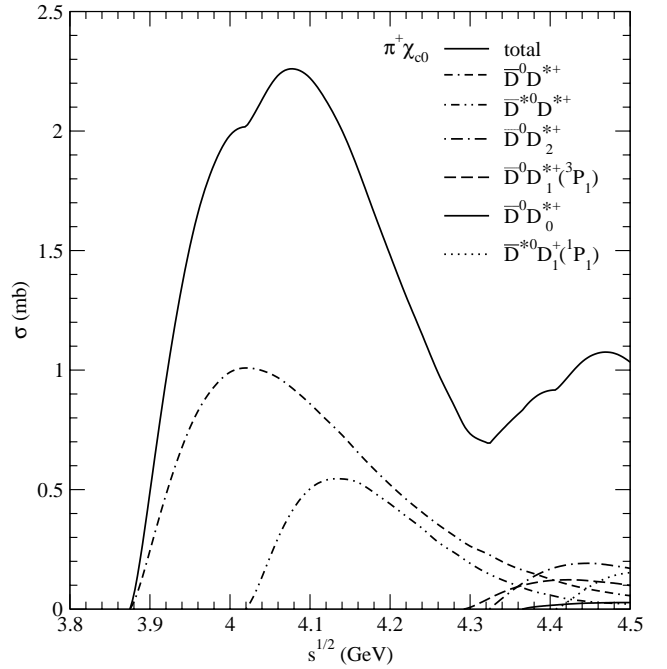


FIG. 3. Same as in Fig. 2, but for $\pi^+ \chi_{c0}$ cross sections.

$$\pi^+ + c\bar{c} \rightarrow \bar{D}^{*0} D^{*+}, \quad (12)$$

$$\pi^+ + c\bar{c} \rightarrow \bar{D}^0 D_2^{*+} + \text{c.c.}, \quad (13)$$

$$\pi^+ + c\bar{c} \rightarrow \bar{D}^0 D_1^{*+}(^3P_1) + \text{c.c.}, \quad (14)$$

$$\pi^+ + c\bar{c} \rightarrow \bar{D}^0 D_0^{*+} + \text{c.c.}, \quad (15)$$

$$\pi^+ + c\bar{c} \rightarrow \bar{D}^{*0} D_1^+(^1P_1) + \text{c.c.} \quad (16)$$

The masses of the \bar{D}^0 , D^{*+} , \bar{D}^{*0} , D^+ , and D_2^{*+} mesons are taken from the 2002 PDG compilation [33]. The D_0^{*+} vector meson is assumed to have a mass of 2.5 GeV. The spin-triplet state $D_1^{*+}(^3P_1)$ and the spin-singlet state $D_1^+(^1P_1)$ mix to form the observed state $D_1(2420)^+$ and another unobserved state [34]. We assume masses for the $D_1^{*+}(^3P_1)$ and $D_1^+(^1P_1)$ of 2.427 and 2.4 GeV, respectively.

The total inelastic cross sections to 4.5 GeV are shown in Figs. 2–8. Results for exclusive reactions are as shown in the figures. The total cross section also includes charge conjugation final states where appropriate.

We note the following general features of the cross sections. All cross sections rise rapidly according to threshold kinematics and subsequently fall off at a scale of Λ_{QCD} as expected for exclusive flavor exchange reactions. The ψ' cross sections are roughly ten times larger than corresponding ψ cross sections. This is in accord with the ratio $r'_{\psi'}/r_{\psi} \approx 2$ and the notion that cross sections increase with hadron size, although we stress that *no simple scaling relationship exists in the quark interchange model*. We note that the ratio of ψ' to ψ is substantially smaller than the factor of 5000 predicted by the Peskin-Bhanot computation [24]. The ψ' cross sections tend to fall more rapidly than those for ψ . We

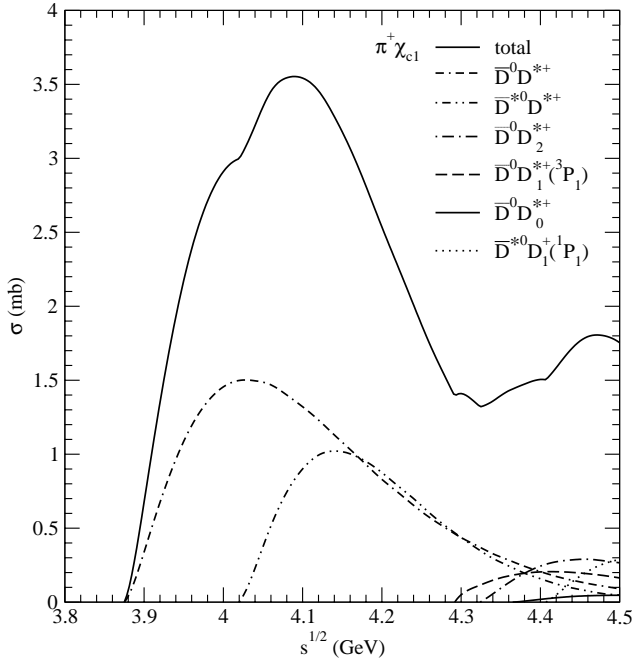


FIG. 4. Same as in Fig. 2, but for $\pi^+ \chi_{c1}$ cross sections.

suspect that this is due to the node in the ψ' radial wave function which manifests itself as a zero in the cross section about 200 MeV above threshold, causing the cross section to drop more rapidly than that for the ground state. Again, this feature can be expected to be quite general. Finally, we note that the χ_{cJ} cross sections grow with angular momentum J , which is naively expected due to the increasing number of J_z states present.

A simple parametrization of these cross sections may prove useful for further numerical investigations. We have

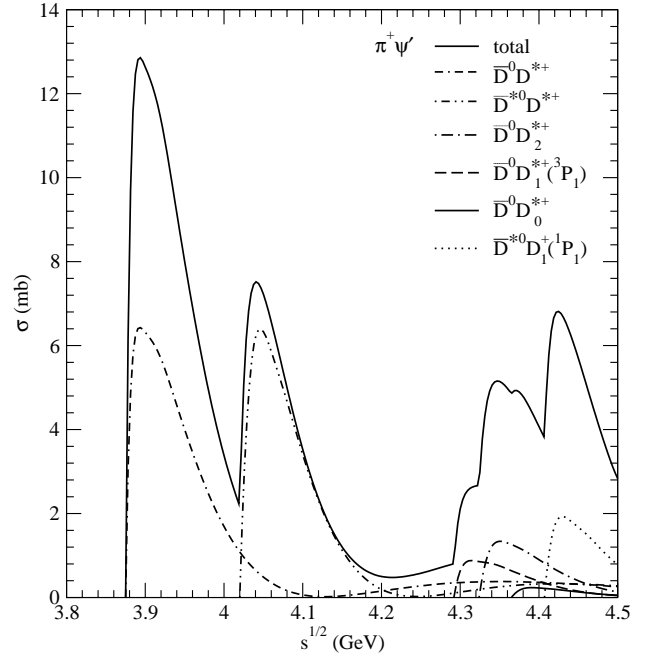


FIG. 6. Same as in Fig. 2, but for $\pi^+ \psi'$ cross sections.

found that it is possible to fit many of our numerical cross sections with a simple functional form which is motivated by the expected threshold behavior with an exponential decay representing suppression due to flavor exchange,

$$\sigma(s) = \sigma_{max} \left(\frac{\epsilon}{\epsilon_{max}} \right)^p \exp[p(1 - \epsilon/\epsilon_{max})], \quad (17)$$

where $\epsilon = \sqrt{s} - M_C - M_D$ and $p = 1/2 + L_{min}^{CD}$ for endothermic reactions and $p = -1/2 + L_{min}^{CD}$ for exothermic reactions. Here

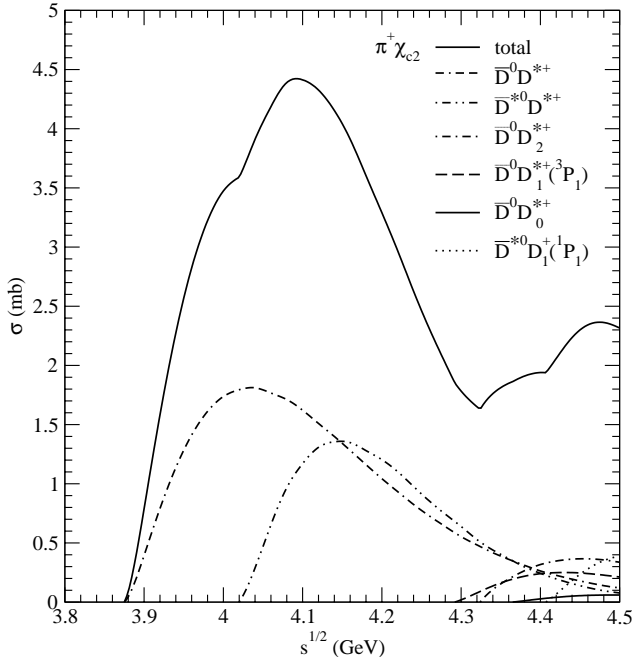


FIG. 5. Same as in Fig. 2, but for $\pi^+ \chi_{c2}$ cross sections.

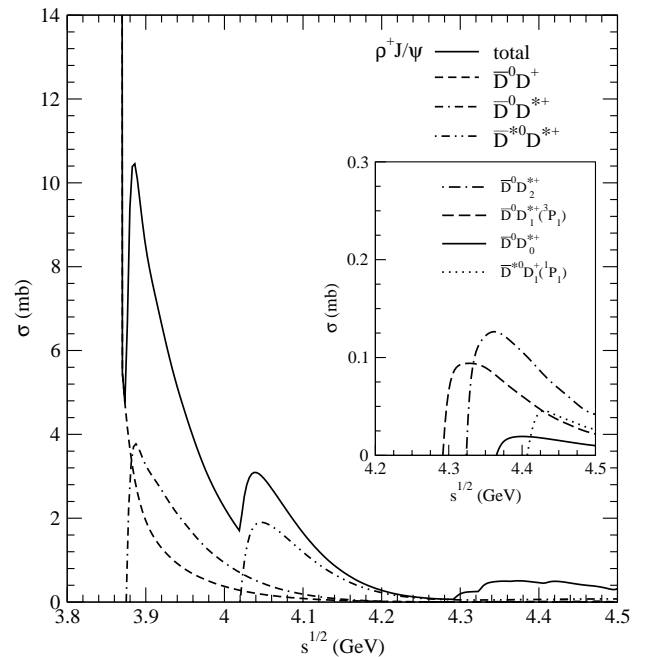


FIG. 7. Same as in Fig. 2, but for $\rho^+ \psi$ cross sections.

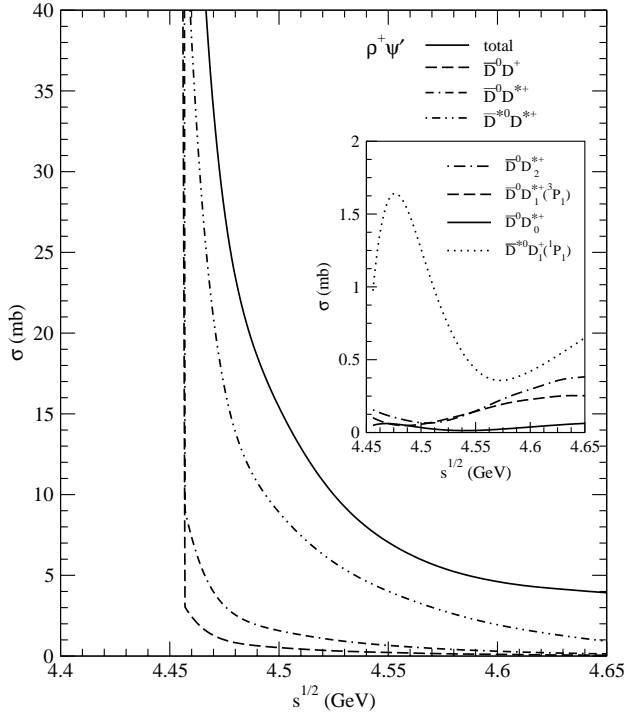


FIG. 8. Same as in Fig. 2, but continued to $\sqrt{s}=4.65$ GeV, and for $\rho^+ \psi'$ cross sections.

L_{min} refers to the minimum possible value for the total orbital angular momentum of the final state consistent with conservation of angular momentum and parity. One expects this to dominate the threshold behavior of a given reaction. In practice, we do find that many cross sections are well

described by assuming that the orbital angular momentum in the initial channel is zero; however, in general many waves contribute, and it is more convenient to simply fit the value of p . We have found that this procedure describes all of our $\pi + c\bar{c}$ reactions quite well (however, this is not true for $\rho + c\bar{c}$). Results for the parameters p , σ_{max} , and ϵ_{max} are presented in the Table I. The D_1^* and D_1 referred to in the column headings represent the $D_1(^3P_1)$ and $D_1(^1P_1)$ states, respectively. All channels except D^*D^* include charge conjugate reactions in the fit parameters.

V. SUMMARY AND CONCLUSIONS

Total charmonium dissociation cross sections have been computed up to 4.5 GeV in the center of mass of the π and $\rho + c\bar{c}$ system. The computations employ standard constituent quark-model dynamics, and all parameters are fixed by spectroscopic data. Exact numerical wave functions have been employed in the computations to minimize post-prior discrepancy. We have also presented results for positive charge conjugation χ_{cJ} dissociation. Gluon fusion arguments indicate that these states should be preferentially produced over negative charge conjugation states in small- x heavy-ion collisions.

It is of interest to speculate on the high-energy limit of these quark-model cross sections. It is apparent from the figures that the cross sections we find for channels that open at higher energies decrease in scale as the channel threshold increases. This is expected since the higher channels have a larger momentum mismatch with the initial state. Thus, exchanged quarks must probe the higher momentum region of the initial hadronic wave functions. This implies that the peaks of high mass channels will be approximately exponen-

TABLE I. Cross section fit parameters.

| | DD^* | D^*D^* | DD_2^* | DD_1^* | DD_0^* | D^*D_1 |
|-----------------------------|--------|----------|----------|----------|----------|----------|
| $\pi J/\Psi \rightarrow$ | | | | | | |
| p | 0.53 | 0.84 | 0.64 | 0.58 | 0.67 | 1.16 |
| σ_{max} | 1.40 | 0.154 | 0.562 | 0.012 | 0.026 | 0.127 |
| ϵ_{max} | 0.059 | 0.044 | 0.074 | 0.050 | 0.050 | 0.052 |
| $\pi \Psi' \rightarrow$ | | | | | | |
| p | 0.67 | 1.17 | 0.84 | 0.74 | 0.83 | 1.42 |
| σ_{max} | 13.04 | 6.30 | 2.66 | 1.78 | 0.466 | 3.81 |
| ϵ_{max} | 0.027 | 0.034 | 0.033 | 0.032 | 0.032 | 0.037 |
| $\pi \chi_{c0} \rightarrow$ | | | | | | |
| p | 1.60 | 1.86 | 1.34 | 1.59 | 0.90 | 2.03 |
| σ_{max} | 2.02 | 0.555 | 0.380 | 0.244 | 0.054 | 0.306 |
| ϵ_{max} | 0.147 | 0.114 | 0.123 | 0.130 | 0.141 | 0.108 |
| $\pi \chi_{c1} \rightarrow$ | | | | | | |
| p | 1.63 | 1.84 | 1.44 | 0.95 | 1.57 | 1.93 |
| σ_{max} | 3.02 | 1.03 | 0.576 | 0.406 | 0.092 | 0.578 |
| ϵ_{max} | 0.154 | 0.122 | 0.130 | 0.120 | 0.132 | 0.114 |
| $\pi \chi_{c2} \rightarrow$ | | | | | | |
| p | 1.65 | 1.84 | 1.10 | 1.52 | 1.36 | 1.89 |
| σ_{max} | 3.64 | 1.37 | 0.724 | 0.598 | 0.122 | 0.790 |
| ϵ_{max} | 0.157 | 0.127 | 0.132 | 0.138 | 0.133 | 0.116 |

tially suppressed in $E_{c.m.}$, due to wave function suppression of the amplitudes. We note that final state hadronic wave functions do not affect this argument, since they are effectively averaged over all length scales near threshold. Furthermore, uncertainties due to relativistic effects or higher Fock state components will not change the argument as long as the momentum transfer probes the confinement region of the wave functions. Uncertainties in the structure of the pion arising from nonperturbative spontaneous chiral symmetry breaking effects are also unimportant here, since the well-understood charmonium wave functions alone suffice to give these general cross section features. Finally, we note that there is an additional suppression due to the nodal structure of highly excited wave functions.

Once the scattering energy is large enough to probe the Coulombic region of the hadronic wave function, we expect to find a power-law suppression of the cross section peak rather than an exponential suppression. This power law is further weakened by the nodal suppression mentioned above. We stress that exclusive cross section peaks must still fall rapidly, even in this perturbative regime.

For two-to-two scattering, the behavior of inclusive cross sections depends on the general behavior noted above and the density of states, which gives the rate at which new channels open with increasing \sqrt{s} . Quark models suggest that the density of $q\bar{q}$ resonances grows as a power of mass, thus the total dissociation cross sections must decrease roughly exponentially while in the confinement regime, and thereafter, as a power in the perturbative regime. At very high energies the gluonic flux tube may be excited, leading to an exponential increase in the density of states [35] since the flux tube contains infinitely many degrees of freedom. However, wave function suppression will again be exponential due to severe suppression of amplitudes containing multiply excited string modes with ground-state string configurations. Thus, for the case of two-body to two-body inclusive flavor-exchange scattering, nonperturbative effects cannot be ignored, and the cross section should decrease with increasing center of mass energy.

The constituent quark model provides a microscopic foundation for the exploration of hadronic interactions at low energy. Thus all relevant reactions may be computed with the addition of no new parameters. This stands in contrast to effective models which must introduce new couplings and form factors, and which suffer from confusion over the correct degrees of freedom and dynamics to be employed (the root problem is that there are no obvious small parameters to guarantee the efficacy of effective Lagrangians in this energy regime). Sum rule and pQCD computations similarly suffer from the notoriously poor convergence properties of QCD (as exemplified in renormalon ambiguities) and from the difficulty in extracting observables from condensates. We regard the constituent quark model as the most reliable tool for the investigation of these issues and in future plan to apply it to charmonium-nucleon scattering and other reactions of interest to the relativistic heavy-ion collider.

ACKNOWLEDGMENTS

We would like to thank our colleagues in the PHENIX Collaboration and at the University of Rostock for discussions on heavy-ion collision physics, and B. Müller for originally suggesting this as a research topic. E.S.S. thanks D. Boyanovsky for discussions of theoretical descriptions of high energy cross sections. The work of Barnes, Wong, and Xu was supported in part by the Division of Nuclear Physics, the U.S. Department of Energy, and by the Laboratory Directed Research and Development Program at the Oak Ridge National Laboratory, under Contract No. DE-AC05-00OR22725 managed by UT-Battelle, LLC. Swanson was supported by the U.S. Department of Energy under Contract Nos. DE-FG02-00ER41135 and DE-AC05-84ER40150, under which the Southeastern Universities Research Association operates the Thomas Jefferson National Laboratory. X.-M.X. thanks the nuclear theory group and the PHENIX group at ORNL for their kind hospitality, and acknowledges additional support from the CAS Knowledge Innovation Project No. KJCX2-SW-N02 and the National Natural Science Foundation of China under Grant No. 10135030.

-
- [1] S.J. Brodsky, G.F. deTeramond, and I.A. Schmidt, Phys. Rev. Lett. **64**, 1011 (1990).
- [2] See, for example, K. Tsushima *et al.*, Phys. Rev. C **59**, 2824 (1999); A. Hayashigaki, Phys. Lett. B **487**, 96 (2000).
- [3] V.A. Novikov, L.B. Okun, M.A. Shifman, A.I. Vainshtein, M.B. Voloshin, and V.I. Zakharov, Phys. Rep. **41**, 1 (1978).
- [4] J.-M. Richard, Nucl. Phys. B, Proc. Suppl. **86**, 361 (2000).
- [5] T. Barnes, N. Black, D.J. Dean, and E.S. Swanson, Phys. Rev. C **60**, 045202 (1999).
- [6] C. Michael and P. Pennanen, UKQCD Collaboration, Phys. Rev. D **60**, 054012 (1999).
- [7] T. Matsui and H. Satz, Phys. Lett. B **178**, 416 (1986).
- [8] K. Martins, D. Blaschke, and E. Quack, Phys. Rev. C **51**, 2723 (1995).
- [9] T. Barnes and E.S. Swanson, Phys. Rev. D **46**, 131 (1992); E.S. Swanson, Ann. Phys. (N.Y.) **220**, 73 (1992). This quark-model approach to calculating hadron-hadron scattering amplitudes has subsequently been applied to $K\pi$, see T. Barnes, E.S. Swanson, and J. Weinstein, Phys. Rev. D **46**, 4868 (1992); NN , see T. Barnes, S. Capstick, M.D. Kovarik, and E.S. Swanson, Phys. Rev. C **48**, 539 (1993); KN , see T. Barnes and E.S. Swanson, *ibid.* **49**, 1166 (1994); BB , see Ref. [5]; and $P\psi$, see Ref. [10].
- [10] T. Barnes, N. Black, and E.S. Swanson, Phys. Rev. C **63**, 025204 (2001). This reference includes a complete list of standard quark-model forces and analytical results for many overlap integrals with Gaussian wave functions.
- [11] C.Y. Wong, E.S. Swanson, and T. Barnes, Phys. Rev. C **62**, 045201 (2000); **65**, 014903 (2001). See also E.S. Swanson, hep-ph/0102267; T. Barnes, E.S. Swanson, and C.Y. Wong, nucl-th/0006012; C.Y. Wong, E.S. Swanson, and T. Barnes, nucl-th/0002034.

- [12] L. I. Schiff, *Quantum Mechanics* (McGraw-Hill, New York, 1968), pp. 384–387. Schiff actually proves that the post-prior ambiguity vanishes, given exact wave functions in the *nonrelativistic* case. Since we use nonrelativistic potential model wave functions but relativistic kinematics, some post-prior ambiguity remains in our results.
- [13] E. Shuryak and D. Teaney, Phys. Lett. B **430**, 37 (1998).
- [14] S.G. Matinyan and B. Müller, Phys. Rev. C **58**, 2994 (1998).
- [15] D. Kharzeev and H. Satz, Phys. Lett. B **334**, 155 (1994).
- [16] Z. Lin, C.M. Ko, and B. Zhang, Phys. Rev. C **61**, 024904 (2000). See also nucl-th/9905007; Z. Lin, T.G. Di, and C.M. Ko, Nucl. Phys. **A689**, 965 (2001).
- [17] Z. Lin and C.M. Ko, Phys. Rev. C **62**, 034903 (2000); J. Phys. G **27**, 617 (2001).
- [18] K. Haglin, Phys. Rev. C **61**, 031902(R) (2000).
- [19] K. Haglin and C. Gale, Phys. Rev. C **63**, 065201 (2001).
- [20] Y. Oh, T. Song, and S.H. Lee, Phys. Rev. C **63**, 034901 (2001).
- [21] F.S. Navarra, M. Nielsen, and M.R. Robilotta, Phys. Rev. C **64**, 021901(R) (2001).
- [22] F.S. Navarra, M. Nielsen, M.E. Bracco, M. Chiapparini, and C.L. Schat, Phys. Lett. B **489**, 319 (2000).
- [23] F.O. Duraes, F.S. Navarra, and M. Nielsen, Phys. Lett. B **498**, 169 (2001).
- [24] M. Peskin, Nucl. Phys. **B156**, 365 (1979); G. Bhanot and M. Peskin, *ibid.* **B156**, 391 (1979).
- [25] M. Peskin (private communication). He notes that this method uses approximations that are not justified even at the Υ mass scale.
- [26] J. Hüfner, Yu.P. Ivanov, B.Z. Kopeliovich, and A.V. Tarasov, Phys. Rev. D **62**, 094022 (2000).
- [27] F. Arleo, P.B. Gossiaux, T. Gousset, and J. Aichelin, Phys. Rev. D **65**, 014005 (2002).
- [28] O. Lakhina and E. S. Swanson (unpublished).
- [29] K. Redlich, H. Satz, and G.M. Zinovjev, Eur. Phys. J. C **17**, 461 (2000).
- [30] F.O. Duraes, H.C. Kim, S.H. Lee, F.S. Navarra, and M. Nielsen, nucl-th/0211092.
- [31] G. A. Schuler, Report No. CERN-TH/94-7170.
- [32] R. Vogt, Phys. Rep. **310**, 197 (1999).
- [33] Particle Data Group, K. Hagiwara *et al.*, Phys. Rev. D **66**, 010001 (2002).
- [34] S. Godfrey and R. Kokoski, Phys. Rev. D **43**, 1679 (1991).
- [35] R. Hagedorn, in *Thermodynamics of Strong Interactions*, edited by E. Schatzman, Cargese Lectures in Physics Vol. 6 (Gordon and Breach, New York, 1973); K. Huang and S. Weinberg, Phys. Rev. Lett. **25**, 895 (1970).